D.B., and D.Y.G. provided reagents and conceptual advice; M.K.E., S.E.C., and K.E. wrote the initial draft of the manuscript; and all authors provided critical review and final approval of the manuscript. All relevant data are within this paper and the supplementary materials. Enteroids are available via a materials transfer agreement from Baylor College of Medicine. Baylor College of Medicine has filed a patent application related to this work: Cultivation of human noroviruses; provisional patent application no. 62/236,294.

SUPPLEMENTARY MATERIALS
www.sciencemag.org/content/353/6306/1387/suppl/DC1
Materials and Methods
Figs. S1 to S11
Table S1
References (*41*–*47*)

25 February 2016; accepted 18 August 2016
Published online 25 August 2016
10.1126/science.aaf5211

NEUROSCIENCE

The TRPM2 channel is a hypothalamic heat sensor that limits fever and can drive hypothermia

Kun Song,[1]*† Hong Wang,[1]† Gretel B. Kamm,[1]† Jörg Pohle,[1] Fernanda de Castro Reis,[2] Paul Heppenstall,[2,3] Hagen Wende,[1] Jan Siemens[1,3]‡

Body temperature homeostasis is critical for survival and requires precise regulation by the nervous system. The hypothalamus serves as the principal thermostat that detects and regulates internal temperature. We demonstrate that the ion channel TRPM2 [of the transient receptor potential (TRP) channel family] is a temperature sensor in a subpopulation of hypothalamic neurons. TRPM2 limits the fever response and may detect increased temperatures to prevent overheating. Furthermore, chemogenetic activation and inhibition of hypothalamic TRPM2-expressing neurons in vivo decreased and increased body temperature, respectively. Such manipulation may allow analysis of the beneficial effects of altered body temperature on diverse disease states. Identification of a functional role for TRP channels in monitoring internal body temperature should promote further analysis of molecular mechanisms governing thermoregulation and foster the genetic dissection of hypothalamic circuits involved with temperature homeostasis.

Core body temperature (T_{core}) is normally maintained very accurately in mammals within a narrow range around 37°C and serves as an important vital sign that is routinely monitored in hospitalized patients. Pathological conditions such as infections and systemic inflammation cause fever (*1*, *2*), an increase in the body's temperature that is thought to be mediated by prostaglandin E_2 (PGE_2)–induced inhibition of warm-sensitive neurons (WSNs) in the hypothalamic thermoregulatory center (*3*). Adverse drug-induced fluctuations in T_{core} can have severe and even fatal consequences (*4*). Conversely, clinically controlled modulation of T_{core} has beneficial effects and can prevent tissue damage, promote trauma recovery (*5*, *6*), or help decrease obesity (*7*).

The preoptic area (POA) of the hypothalamus serves as a thermostat, integrating temperature information to orchestrate the autonomous and behavioral adaptations needed to achieve thermal homeostasis (*3*, *8*). POA neurons receive and integrate information from peripheral temperature sensors located in the skin, spinal cord, and viscera. Local POA warming and cooling experiments (*9*–*13*) and genetic manipulations (*14*) have shown that this region of the central nervous system also detects local brain temperature changes, which have a strong impact on T_{core}. In fact, temperature changes in the POA can exert a dominant effect on T_{core} and can override lower-priority temperature inputs from peripheral temperature sensors, such as those located in the skin (*15*, *16*). Warming of the POA induces heat dissipation mechanisms such as cutaneous vasodilation, evaporative heat loss mechanisms, and behavioral adaptations, whereas cooling of the POA triggers heat conservation and thermogenesis.

POA neurons exhibiting pronounced temperature sensitivity have been described in in vivo models and in vitro preparations (*17*–*19*). WSNs enhance their firing rate upon warming, a process that is thought to relay temperature information to peripheral organs to promote heat loss (*3*). Conversely, a drop in deep brain temperature inhibits WSNs, a process that correlates with induction of thermogenesis and heat gain.

However, the genetic identity of WSNs and the molecular basis of their temperature sensitivity have remained elusive. Our work defined a population of WSNs that controls temperature homeostasis and identified a transient receptor potential (TRP) ion channel that subserves thermodetection in hypothalamic neurons.

TRPM2 is a heat sensor in a subset of POA neurons

To identify thermosensory molecules in the thermoregulatory center of the hypothalamus, we established calcium imaging as a means to monitor warming-induced responses of primary POA neuronal cultures (fig. S1, A to F). We applied a stringent criterion to identify WSNs by fura-2–mediated calcium imaging. We only counted neurons as WSNs if their relative increase in signal on receiving a thermal stimulus (up to 45°C) was larger than the mean fura-2 signal plus 5 times the standard deviation (5SD) of thermally unresponsive human embryonic kidney–293 cells subjected to the same temperature stimulus (fig. S1, E and F). This procedure allowed us to account and correct for the small unspecific temperature effect on the fluorescent fura-2 signal (*20*) (see fig. S1F and table S1 for details). We found that 16.3 ± 4.7% (mean ± SEM; n = 6 mice) of cultured POA neurons responded to warming, a fraction that is in the same range (10 to 16%) observed in electrophysiological studies of rodent POA cultures (*21*, *22*) and slightly lower than WSN percentages (20 to 40%) observed in POA slice preparations (*17*, *23*). Extracellular calcium appeared to be the source of the temperature-triggered increase in intracellular concentrations of free calcium, because chelation of external calcium abolished the response, whereas depletion of intracellular calcium stores did not have any effect on warm sensitivity (fig. S1, D and G).

Several ion channels are thermosensitive, exemplified by a steep temperature dependence (Q_{10} coefficient) of their opening probabilities. In particular, cationic TRP ion channels have been identified as thermosensors in the peripheral nervous system and function in the detection of ambient temperature changes (*24*–*27*).

To identify candidate channels mediating the observed warm sensitivity in neuronal POA cultures, we tested various inhibitors and agonists of TRPs and other thermosensitive ion channels (fig. S1, H to L). The calcium response appeared to be mediated by direct Ca^{2+} flux through a thermosensitive ion channel and not an indirect readout of voltage-gated channels, because nifedipine and tetrodotoxin, which are blockers of voltage-gated calcium and sodium channels, respectively, had only a small effect on the responses to increased temperature (fig. S1, H, J, K, and L). 2-aminoethoxydiphenyl borate (2-APB), a potent inhibitor of several ion channels and activator of TRPV-type channels (*28*–*30*), abolished the temperature response of POA neurons in a reversible manner (Fig. 1A).

[1]Department of Pharmacology, University of Heidelberg, Im Neuenheimer Feld 366, 69120 Heidelberg, Germany. [2]European Molecular Biology Laboratory (EMBL), Adriano Buzzati-Traverso Campus, Via Ramarini 32, 00016 Monterotondo, Italy. [3]Molecular Medicine Partnership Unit, EMBL, Meyerhofstraße 1, 69117 Heidelberg, Germany. *Present Address: Max Delbrück Center for Molecular Medicine, Robert Rössle Straße 10, 13125 Berlin, Germany. †These authors contributed equally to this work. **‡Corresponding author. Email: jan.siemens@pharma.uni-heidelberg.de**

Among known temperature-responsive ion channels, TRPC5, TRPM2, TRPM3, TRPM8, TRPV1, TRPV2, TRPV3, and STIM1-ORAI1 are sensitive to 2-APB (fig. S1M) (*24*–*26*). Because TRPC5 and TRPM8 are cold-sensitive channels (*31*–*33*), we eliminated them from our list of candidates. The STIM1-ORAI1 channel complex responds to cooling subsequent to a heat stimulus (*34*), a characteristic that differs from the POA responses described here.

The TRPV1 to -3 channels are activated rather than inhibited by 2-APB (*28*, *35*), and capsaicin, the cognate agonist of heat-sensitive TRPV1, did not have any effect on POA neurons (fig. S1N), suggesting that TRPV1 to -3 do not serve as temperature sensors in POA neurons. Moreover, these channels are sensitive to the pore blocker ruthenium red (*36*), a substance that had only a subtle effect on the temperature sensitivity of POA neurons (fig. S1, I and L).

TRPM3, one of the two remaining candidates, appeared to be expressed in the POA, albeit in low amounts, as assessed by in situ hybridization (fig. S1O). However, the TRPM3 agonist pregnenolone sulfate did not produce calcium responses in neuronal POA cultures (fig. S1N). It did so in dorsal root ganglia sensory neurons that express the receptor (*37*), which we used as a positive control.

Immunohistochemistry and in situ hybridization for TRPM2 showed prominent labeling within the mouse POA (Fig. 1, B and C, and fig. S3, B and C). H_2O_2, a sensitizer of TRPM2 channel activity (*38*), shifted the warm sensitivity of POA cultures to a lower activation temperature (Fig. 1D). Moreover, adenosine diphosphate ribose (ADPR), an intracellular agonist of TRPM2 (*39*, *40*), induced large currents in POA neurons that were identified by calcium imaging to be warm-sensitive (Fig. 1, E and F, and fig. S1, P to S). The ADPR-induced current showed a TRPM2-characteristic linear current-voltage relationship (*39*, *40*). Additionally, a similar current was induced in these neurons by increased temperatures (Fig. 1F).

Thus, TRPM2 may mediate responses to temperature increases in the POA. To test this, we used cultures obtained from *Trpm2*$^{-/-}$ mice (*41*) and compared their thermal responses with those from wild-type (*Trpm2*$^{+/+}$) littermate controls. The magnitude of the response of POA neurons to increased temperature was decreased in the absence of TRPM2, and these neurons were indistinguishable from warm-insensitive (non-WSN) *Trpm2*$^{+/+}$ POA neurons (Fig. 1, G and H). Using our stringent definition of warm sensitivity (fig. S1F), no responses to increased temperatures were detected in cultures obtained from *Trpm2*$^{-/-}$ mice (Fig. 1I).

The activation temperature of cultured WSNs—in the absence of a sensitizer such as H_2O_2 or any other reactive oxygen species—was in the range of 45°C (fig. S2A). Although this temperature is similar to that previously reported for TRPM2 activation (*38*), it exceeds any physiologically relevant deep brain temperature, even when compared with extreme forms of fever and hyperthermia (*42*). However, similar to other thermosensitive TRP channels, the activation temperature for TRPM2 appears not to be a fixed threshold temperature. Rather, it ranges from 33° to 47°C, depending on the cellular context (*38*, *43*). We therefore tested whether the activation temperature of POA neurons shifted to lower, more physiological temperatures when calcium imaging was performed on acutely obtained brain slices from 7- to 8-week-old mice. In this experimental setting, the neurons largely retained their native cellular environment and had attained maturity.

To this end, we injected virus particles into the mouse POA for Cre-dependent expression of the virally encoded intracellular calcium indicator GCaMP6, which shows increased fluorescence

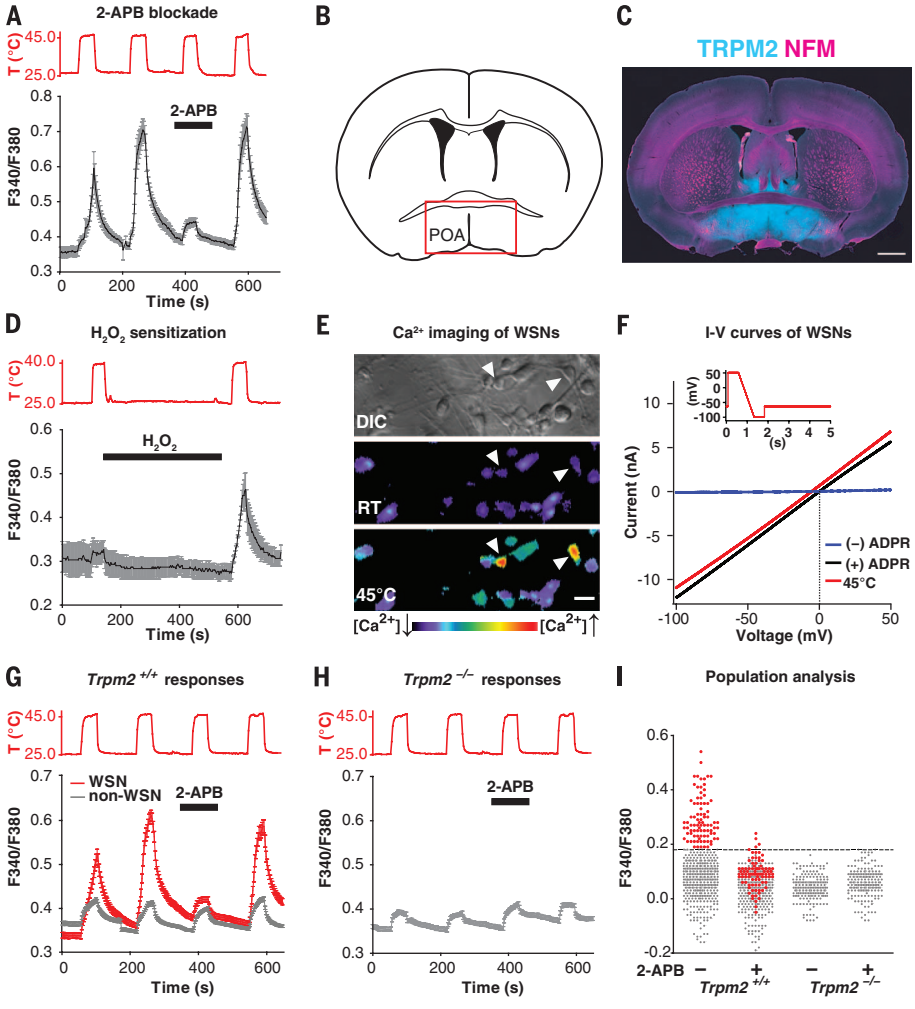

Fig. 1. TRPM2 mediates heat responses in a subset of POA neurons. (**A**) Cultured mouse POA neurons were examined for calcium responses [black trace; plotted are non-normalized fura-2 fluorescence intensity ratios after excitation at 340 and 380 nm (F340/F380)] to repetitive increases in temperature (red trace). 2-APB (30 μM, black bar) reversibly blocked thermal responses in POA neurons. (**B**) Cartoon depicting a coronal section of a mouse brain (Bregma level anterior-posterior, 0.14 mm). (**C**) Immunostaining of a representative mouse brain section corresponding to the cartoon in (B), using antibodies against TRPM2 (cyan) and neurofilament medium (NFM, magenta). Scale bar, 1 mm. (**D**) H_2O_2 (1 mM, black bar) sensitized POA neurons to respond to lower activation temperatures (40°C), as assessed by fura-2–based calcium imaging (black trace). (**E**) Differential interference contrast (DIC) image (top) and fura-2 ratio images before (middle; RT, room temperature) and during (bottom) a temperature stimulus of cultured POA neurons. Arrowheads indicate WSNs. (**F**) Current-voltage (*I-V*) relationships of voltage-clamped WSNs shown in (E) in response to a voltage ramp shown at the top, in the absence (blue) or presence (black) of ADPR (100 μM) or at a temperature stimulus of 45°C (red). (**G** and **H**) POA cultures from *Trpm2*$^{+/+}$ (G) and *Trpm2*$^{-/-}$ (H) mice were examined by calcium imaging for responses to repetitive thermal stimuli (upper red traces) in the presence or absence of 2-APB (30 μM, black bar). In *Trpm2*$^{+/+}$ cultures, both WSNs (red) and non-WSNs (light gray) could be detected, whereas WSNs were absent in cultures of *Trpm2*$^{-/-}$ mice. (**I**) Population analysis of thermal responses of POA neurons from *Trpm2*$^{+/+}$ and *Trpm2*$^{-/-}$ mice as shown in (G) and (H). Plotted are the peak responses of individual neurons at the second (without 2-APB) and third (with 2-APB) temperature stimulus. POA neurons of both genotypes had similar responses to a high-potassium solution (100 mM KCl, not shown). WSNs are colored in red and non-WSNs in gray. The dashed line demarcates the cutoff for warm sensitivity as defined in fig. S1F and table S1. Throughout, error bars indicate SEM.

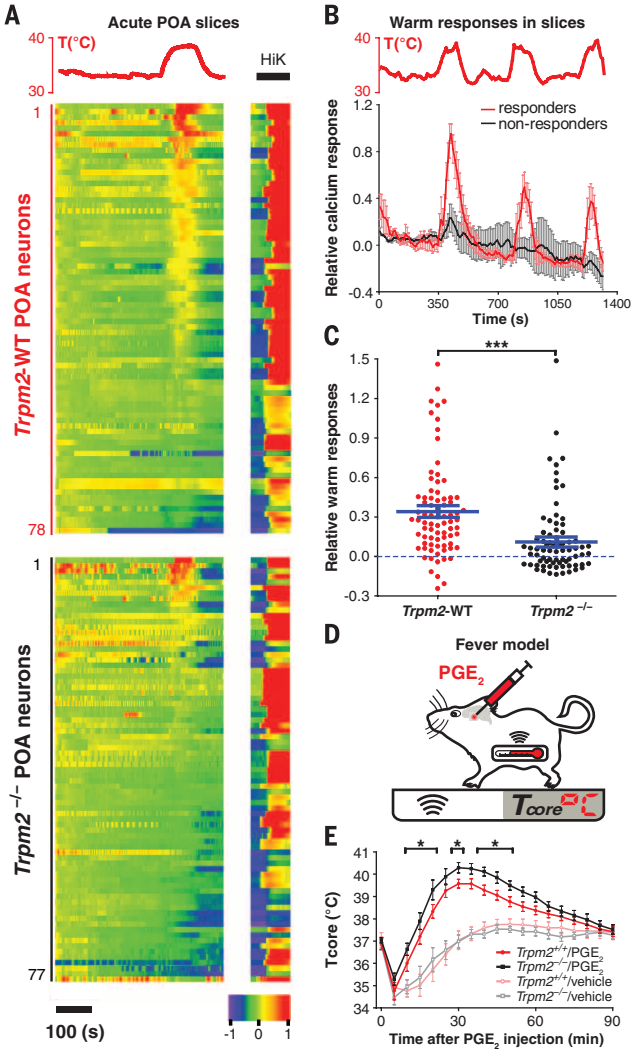

Fig. 2. TRPM2 mediates heat responses in POA brain slices and modulates fever temperature in vivo. (**A**) Acute POA slice preparations from *Nestin-Cre* mice with (*Trpm2*-WT; upper panel) or without (*Trpm2*$^{-/-}$; lower panel) functional TRPM2 were consecutively subjected to a temperature stimulus of 38 ± 1°C (red) and a high-potassium stimulus (HiK, black). Neuronal activity was recorded by means of a Cre-induced, virally encoded GCaMP6 calcium sensor that was stereotactically introduced into the POA 2 weeks before slice preparation. A nonlinear pseudocolor scale (bottom) indicates relative calcium responses in individual neurons. Numbering on the left refers to individual neurons. The black bar indicates the time scale. (**B**) Average relative calcium responses of exemplary GCaMP6^{+} WSNs (red; n = 5) and non-WSNs (black; n = 3) from *Nestin-Cre* mice to repetitive temperature stimuli of up to 40°C (top, red trace). (**C**) Population analysis of cellular responses shown in (A), demonstrating that relative heat-induced calcium signals are reduced in POA slices from mice lacking functional TRPM2 (***P < 0.0001, two-tailed Mann-Whitney test). Blue bars show the mean and SEM. (**D**) Cartoon depicting the experimental paradigm used to examine the fever response by thermotelemetrical measurements of T_{core} upon preoptic injection of PGE_2 into the POA. (**E**) Enhanced PGE_2-induced fever in *Trpm2*$^{-/-}$ mice (black trace; n = 9) compared with littermate *Trpm2*$^{+/+}$ controls (red trace; n = 10). Mice were briefly anesthetized to allow stereotactic injection of PGE_2 (or vehicle control), resulting in a transient drop of T_{core} for all conditions and genotypes. *P < 0.05, two-way analysis of variance (ANOVA) ($F_{1,318}$ = 40.78) followed by post hoc Fisher's least significant difference (LSD) test.

at 500 to 530 nm upon an increase in cytosolic calcium levels (*44*). To test temperature sensitivity in POA neurons, we used the neuron-specific *Nestin-Cre* mice (*45*) that express Cre recombinase, and thus GCaMP6, in POA neurons. Subsequent temperature stimulation of brain slices prepared from these animals revealed calcium responses in POA neurons at 38 ± 1°C (Fig. 2, A and B). Moreover, POA neurons in slices derived from mice lacking TRPM2 (*Nestin-Cre Trpm2*$^{-/-}$) had attenuated responses to the same temperature stimulus [mean relative heat responses ± SEM: *Nestin-Cre Trpm2*$^{-/-}$, 0.111 ± 0.033 (n = 78); *Nestin-Cre Trpm2*-WT, 0.341 ± 0.040 (n = 79); P < 0.0001, two-tailed Mann-Whitney test; *Trpm2*-WT signifies *Trpm2*$^{+/+}$ and *Trpm2*$^{+/-}$ mice] (Fig. 2, A and C, and fig. S2B). General excitability, as assessed by high potassium stimulation, was indistinguishable in the presence or absence of TRPM2 (fig. S2C). These results demonstrate that preoptic TRPM2 mediates responses to heat stress at temperatures of (or exceeding) 38°C.

Preoptic TRPM2 receptors modulate the magnitude of fever temperature

Fever is a cardinal response to infection and systemic inflammation. The POA, as part of its thermoregulatory function, is the key brain structure in controlling the increased body temperature in fever (*2*, *3*). The TRPM2-mediated activation of POA neurons at stimulation temperatures slightly above the physiological set point of 37°C (sometimes referred to as the balance point), might allow hypothalamic TRPM2 to detect and modulate inflammatory fever temperature.

As a consequence of infection and downstream of the resulting immune response, PGE_2 is the final mediator that triggers fever by acting directly on POA neurons (*2*, *46*). To address a putative fever-modulatory role for TRPM2 directly in the POA, we microinjected PGE_2 into this brain area in mice (Fig. 2D and fig. S2D), an established fever model (*46*–*48*). Telemetrically measured T_{core} revealed similar diurnal temperatures in the presence and absence of TRPM2 at normothermic (nonfever) conditions (fig. S2E). We found that injection of a low dose of PGE_2 (0.4 nmol per mouse) produced a mild fever response that was similar in both genotypes (fig. S2, F and I). However, a high dose of PGE_2 (4 nmol per mouse) caused an increased fever temperature in *Trpm2*$^{-/-}$ mice compared with that of *Trpm2*$^{+/+}$ littermate controls (Fig. 2E and fig. S2I). In the absence of functional TRPM2 protein, the maximal fever temperature reached 40.4 ± 0.2°C, compared with 39.6 ± 0.2°C in the presence of the receptor (n = 9 *Trpm2*$^{-/-}$ and 10 *Trpm2*$^{+/+}$ mice; P < 0.001, two-tailed unpaired t test).

We also tested the effects of the interleukins IL-1β and IL-6, which have been shown to synergistically induce fever at central sites (*49*). Again, significantly higher fever was detected in *Trpm2*$^{-/-}$ mice only for the stronger of the two stimuli, when both interleukins were co-injected into the POA, but not when IL-1β was injected alone (fig. S2, G to I). Together, these results indicate that preoptic TRPM2 limits the magnitude of the temperature increase in strong fever responses, presumably to prevent excessive temperature increases and tissue damage.

Trpm2-expressing POA neurons are part of a circuit controlling body temperature homeostasis

Our results indicated that *Trpm2*-expressing (*Trpm2*$^{+}$) neurons might be part of a thermoregulatory circuit and that TRPM2-driven activity might counteract body heating and perhaps promote peripheral heat loss at normothermic conditions as well. In the absence of specific agents to modulate TRPM2 function in vivo, we generated *Trpm2-2A-Cre* knock-in mice (referred to hereafter as *Trpm2-Cre* mice) that express Cre recombinase exclusively in *Trpm2*$^{+}$ cells (fig. S3A). We thereby gained genetic access to *Trpm2*$^{+}$ POA neurons and ascertained the potential thermoregulatory role of this specific cell population in unrestrained, conscious mice. We first assessed proper *Cre* expression in *Trpm2*$^{+}$ neurons, using in situ hybridization and *Cre* reporter mice. *Cre* was expressed in the POA of *Trpm2-Cre* mice, and its expression pattern recapitulated that of native *Trpm2* transcripts (fig. S3, B to F). Two-color in situ hybridization analysis of the POA revealed essentially complete cellular overlap of *Trpm2* and *Cre* (fig. S3F), with 97% of *Trpm2*$^{+}$ neurons (335 out of 344 cells) expressing the Cre-induced reporter.

We then tested whether modulating the activity of *Trpm2*$^{+}$ POA neurons influenced body temperature in freely moving mice. We chose a chemogenetic, DREADD (designer receptors exclusively activated by designer drugs) receptor–assisted approach that enabled us to remotely turn the activity of *Trpm2*$^{+}$ neurons on and off.

DREADDs are engineered heteromeric guanine nucleotide–binding protein (G protein)–coupled receptors that are activated by the otherwise inert drug clozapine-*N*-oxide (CNO) and couple to different G protein signaling cascades that either activate (Gq-DREADD) or inhibit (Gi-DREADD) neuronal activity (*50*). We injected viral constructs encoding Cre-dependent ("flexed") DREADD receptor expression cassettes (*51*) into the POA of *Trpm2-Cre* mice (Fig. 3A). This allowed the specific activation or inhibition of *Trpm2-Cre*$^+$ POA neurons through systemic application of CNO. No expression of DREADDs occurred in the absence of Cre recombinase.

To verify the capacity of CNO to exert control over *Trpm2*$^+$ neurons in vitro, we co-infected POA neurons by stereotactic injection of Cre-inducible DREADD receptors and GCaMP6 viral constructs into *Trpm2-Cre* mice. In brain slices derived from these mice, the respective DREADD receptor and GCaMP6 are coexpressed in *Trpm2*$^+$ neurons. Calcium imaging of POA neurons expressing Gq-DREADD or Gi-DREADD together with GCaMP6 confirmed that CNO application activated or inhibited *Trpm2*$^+$ neurons, respectively (fig. S3G).

We implanted telemetric temperature probes in the peritoneal cavity of DREADD-virus–injected *Trpm2-Cre* mice to permit recording of T_{core} in conscious, unrestrained animals (Fig. 3B). Diurnal body temperature regulation of DREADD-infected *Trpm2-Cre* mice in the absence of CNO was similar to that of control animals (fig. S3H). In contrast, CNO-mediated activation of *Trpm2*$^+$ POA neurons resulted in a sustained decrease in body temperature (Fig. 3, C to E, and fig. S3I). T_{core} dropped to 27.4 ± 0.6°C when *Trpm2*$^+$ neurons were activated in Gq-DREADD–infected mice but not in control-infected or saline-injected mice.

The temperature decrease correlated with a reduction in activity of the animals and was also reflected by a temperature drop of the body shell, as visualized by infrared (IR) imaging (Fig. 3F and movie S1). The hypothermic state lasted several hours (0.3 mg/kg of CNO induced hypothermia for 12.5 ± 2.4 hours) and could be induced repetitively without causing any apparent long-term adverse effects (Fig. 3E).

The animal's tail, an important thermal effector organ controlling heat dissipation (*3*, *52*), showed an increase in surface temperature of 3.7 ± 0.5°C that coincided with the overall heat loss (Fig. 3, F and G; fig. S3J; and movie S1), demonstrating that *Trpm2*$^+$ POA neurons drive hypothermia by triggering cutaneous vasodilation. Additionally, stimulation of *Trpm2*$^+$ neurons prevented activation of interscapular brown adipose tissue (BAT; fig. S3K), which normally mediates thermogenesis when the body cools.

Conversely, Gi-DREADD receptor–mediated inhibition of *Trpm2*$^+$ POA neurons resulted in a significant temperature increase, reaching a T_{core} of up to 39.1 ± 0.1°C (Fig. 3H and fig. S3I), suggesting that under normothermic conditions, *Trpm2*$^+$ neurons in the POA are tonically active. This is in agreement with previous electrophysiological recordings that show tonic ongoing activity of WSNs (*17*–*19*). Gi-DREADD–mediated neuronal inhibition had no significant effect on tail vasomotor tone at ambient temperature (~20°C), likely because the prominent vasoconstriction that prevails under these conditions (*53*) precludes detection of any further reduction of the IR signal (Fig. 3G). These results demonstrate that *Trpm2*$^+$ neurons in the POA are part of a circuit that orchestrates thermal effector processes to modulate T_{core} homeostasis.

Excitatory *Trpm2*$^+$ neurons drive hypothermia

WSNs in the POA have been proposed to be γ-aminobutyric acid (GABA)–releasing neurons that exert their effect largely by inhibiting downstream components of the thermoregulatory circuit (*3*). We therefore used two-color in situ hybridization on *Trpm2-Cre* reporter mice to ascertain whether *Trpm2*$^+$ neurons are of inhibitory or excitatory origin. We used in situ probes for transcripts encoding the vesicular glutamate transporter 2 (VGLUT2) and glutamate decarboxylase 1 (GAD1), which are excitatory and inhibitory markers, respectively (*54*) (Fig. 4A).

By this analysis, 30 ± 1% of *Trpm2*$^+$ POA neurons were excitatory (*Vglut2*$^+$) neurons, whereas 57 ± 7% coexpressed the inhibitory marker *Gad1* (mean ± SEM; n = 3 mice) (Fig. 4A and fig. S4A). We therefore tested whether activation of the excitatory or inhibitory neuronal population within the POA recapitulated the strong thermoregulatory phenotype observed on activation of *Trpm2*$^+$ neurons (Fig. 3, C to G). *Vgat-Cre* (*54*) and

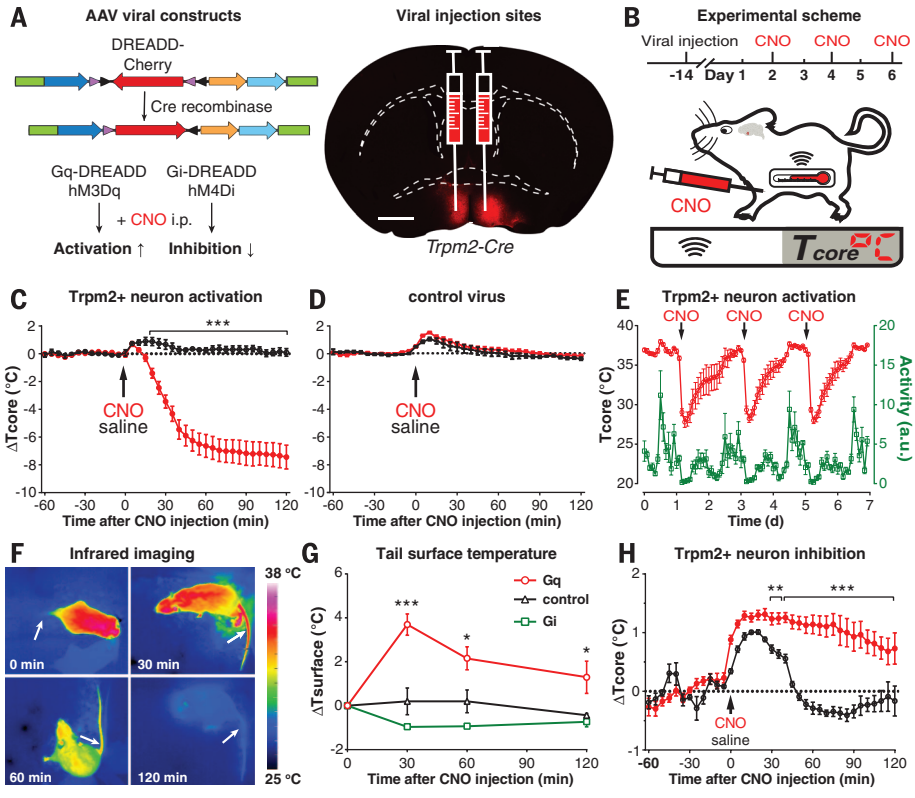

Fig. 3. Control of core body temperature by *Trpm2*$^+$ POA neuron activity. (**A**) Virally encoded, Cre-inducible DREADD-receptor–cherry fusion proteins (left panel) were bilaterally injected into the POA of *Trpm2-Cre* mice and visualized by fluorescent microscopy (right panel). The red arrows indicate the orientation of the DREADD–cherry cDNA reading frame; i.p., (injected) intraperitoneally. (**B**) Illustration detailing the experimental paradigm for examining the impact of *Trpm2*$^+$ neuronal activity on T_{core}. (**C** to **E**) CNO (0.3 mg/kg; red) or vehicle (saline; black) was intraperitoneally injected into mice infected with Gq-DREADD [(C) and (E)] or control virus (D), and T_{core} and activity [green trace in (E)] were measured telemetrically. Arrows indicate the time of injection. a.u., arbitrary units. (**F**) IR thermal imaging of *Trpm2-Cre* mice preoptically expressing Gq-DREADD in *Trpm2*$^+$ neurons, before (0 min) or at indicated time points after CNO injection, revealed pronounced cutaneous heat dissipation through tail vasodilation (arrows). (**G**) Change in tail temperature over time [(arrows in (F)] in *Trpm2-Cre* mice infected with Gq-DREADD (red), saline control (black), or Gi-DREADD (green) upon CNO treatment. (**H**) CNO-mediated inhibition of *Trpm2*$^+$ neurons in Gi-DREADD–infected *Trpm2-Cre* mice showed an oppositely directed effect compared with that in Gq-DREADD–infected animals (C) and resulted in a significant increase in T_{core}. The arrow indicates the time of injection. Telemetry data [(C), (D), and (H)]: Gq-DREADD $F_{1,6} = 75.6$, ***$P < 0.0001$; control virus $F_{1,6} = 1.55$; Gi-DREADD $F_{1,6} = 38.5$, **$P < 0.01$, ***$P < 0.0001$. IR imaging (G): Gq-DREADD $F_{1,5} = 9.3$, *$P < 0.05$, ***$P < 0.001$; Gi-DREADD $F_{1,4} = 5.2$; two-way ANOVA followed by post hoc Fisher's LSD test (n = 4 mice per group). P values indicate significance of the post hoc test.

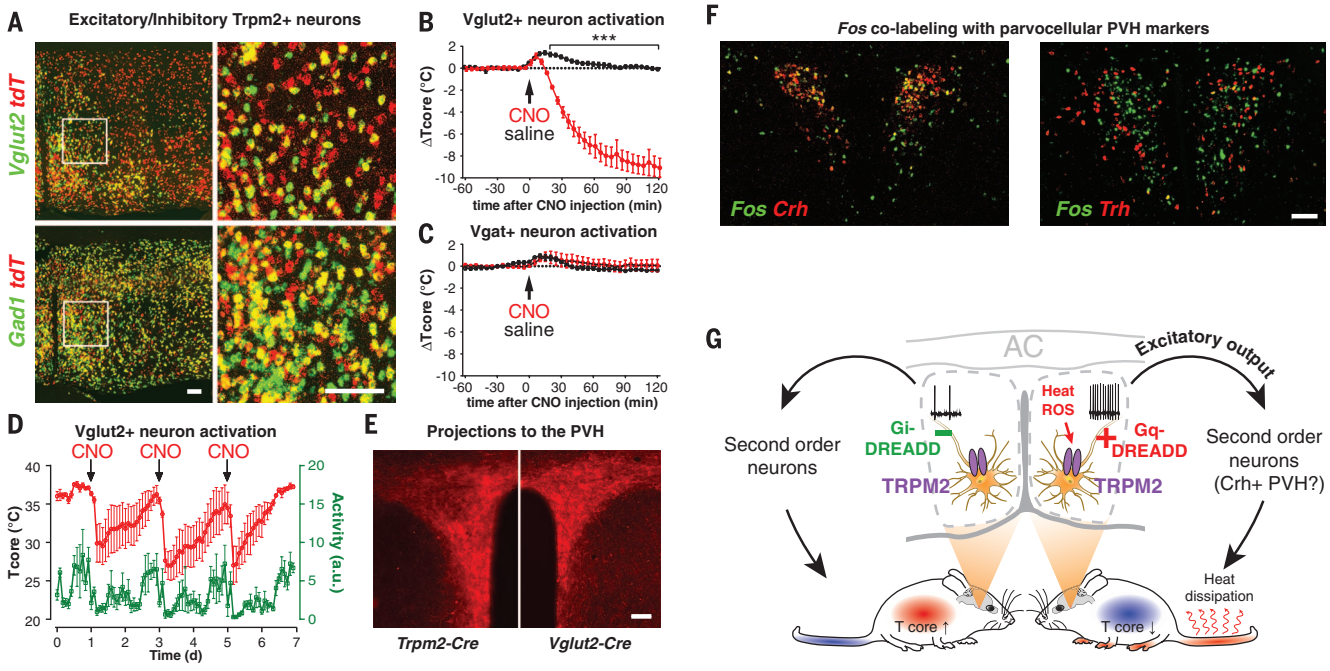

Fig. 4. Stimulation of preoptic *Vglut2*$^+$ neurons recapitulates *Trpm2*$^+$ neuron–driven hypothermia and activates *Crh*$^+$ neurons in the PVH. (**A**) Representative two-color in situ hybridizations of coronal brain sections from *Trpm2-Cre* mice crossed with a *Cre* reporter expressing *tdTomato* (*tdT*) with probes detecting *tdT* (red) and *Gad1* or *Vglut2* (green). The right panels show close-up views indicated by the boxes in the left panels. (**B** to **D**) *Vglut2-Cre* mice and *Vgat-Cre* mice were bilaterally injected with Gq-DREADD virus and subjected to the same experimental paradigm as shown in Fig. 3B. Arrows indicate the time of injection. CNO-mediated activation of *Vglut2-Cre* mice [(B) and (D)], but not *Vgat-Cre* mice (C), recapitulated *Trpm2*$^+$ neuron–driven hypothermia both in magnitude (B) and kinetics (D). *Vglut2-Cre* $F_{1,6} = 86.08$, $^{***}P < 0.0001$; *Vgat-Cre* $F_{1,4} = 0.44$; two-way ANOVA followed by post hoc Fisher's LSD test ($n = 4$ *Vglut2-Cre* and 3 *Vgat-Cre* mice). (**E**) Representative fluorescent images of brain sections from *Vglut2-Cre* and *Trpm2-Cre* mice preoptically expressing Gq-DREADD–cherry fusion protein (Fig. 3A), showing cherry$^+$ fibers projecting to the PVH. (**F**) Two-color fluorescent in situ hybridizations of brain sections from *Vglut2-Cre* mice preoptically expressing Gq-DREADD, using probes to detect *Fos* (green) and *Crh* or *Trh* (red). The animals were injected with CNO 30 minutes before preparation of the tissue sections. Neuronal activation of *Crh*$^+$ neurons but not *Trh*$^+$ neurons in the PVH was detected. (**G**) Model depicting *Trpm2*$^+$ POA neurons and their bidirectional effect on T_{core}. Heat (and reactive oxygen species, ROS) activate TRPM2 to depolarize WSNs, a process that can be mimicked by exogenous Gq-DREADD activation. Increased WSN activity (black traces) triggers an excitatory pathway that promotes heat loss and hypothermia, possibly through a circuit involving *Crh*$^+$ neurons in the PVH. Conversely, inhibiting *Trpm2*$^+$ neurons results in an elevation of T_{core}. AC, anterior commissure. *P* values indicate significance of the post hoc test. All scale bars, 100 μm.

Vglut2-Cre (*55*) mice have been used previously to label inhibitory and excitatory hypothalamic neurons, respectively. Thus, T_{core} recordings of Gq-DREADD–injected *Vgat-Cre* and *Vglut2-Cre* mice were acquired, and viral expression in the respective POA neurons was later verified (fig. S4, B and C). CNO activation of *Vglut2*$^+$ neurons but not *Vgat*$^+$ neurons reproduced the prolonged drop in T_{core} (Fig. 4, B to D), indicating that excitatory, *Trpm2*$^+$ neurons mediate the strong thermoregulatory effect. *Vglut2*$^+$ neuron–driven hypothermia could be induced repetitively and was well tolerated by the animals (Fig. 4D), similar to observations for in vivo chemogenetic activation of preoptic *Trpm2*$^+$ neurons (Fig. 3E). In situ hybridization revealed that Cre recombinase in the *Vglut2-Cre* line was expressed only in ~20% of all *Vglut2*$^+$ POA neurons (fig. S4D). This indicates that activation of a subpopulation of *Vglut2*$^+$ POA neurons, making up only ~6% of all preoptic *Trpm2*$^+$ neurons (fig. S4A), is sufficient to mediate the strong hypothermic effect (Fig. 4, B and D).

Thermoregulatory signals arising from the POA are channeled to different peripheral effector organs through discrete hypothalamic and extrahypothalamic output nuclei (*3*). Given the overlapping expression pattern of *Vglut2* and *Trpm2* in the POA and a similar capacity of both neuron groups to trigger hypothermia on activation, we reasoned that axons of both neuron cohorts might converge on the same downstream output nucleus. Projections of *Cre*-expressing POA neurons were labeled with fluorescent reporters that were introduced together with the DREADD expression cassette by viral infection of the POA area (Fig. 3A). POA infections of *Trpm2-Cre* and *Vglut2-Cre* mice resulted in prominent labeling of fibers terminating in the paraventricular nucleus of the hypothalamus (PVH) (Fig. 4E), a region not previously identified as a major thermoregulatory outlet (*3*). Moreover, CNO administration in *Trpm2-Cre* and *Vglut2-Cre* mice harboring Gq-DREADD–infected POA neurons resulted in DREADD-specific expression of *Fos* in the PVH, demonstrating that *Trpm2*$^+$ *Vglut2*$^+$ POA neurons can excite PVH neurons (fig. S4E). Corticotropin-releasing hormone–positive (*Crh*$^+$) neurons in the PVH are part of the hypothalamic-pituitary-adrenal (HPA) stress response system, which is also activated in response to fever (*56*). We found that DREADD-mediated activation of *Vglut2*$^+$ POA neurons specifically excites parvocellular *Crh*$^+$ neurons but not neighboring thyrotropin-releasing hormone–positive (*Trh*$^+$) neurons or magnocellular vasopressin$^+$ and oxytocin$^+$ PVH neurons (Fig. 4F and fig. S4F). Of all *Fos*$^+$ neurons, we found that 88.4 ± 1.5% (mean ± SEM; $n = 3$ mice) are *Crh*$^+$.

Collectively, these results indicate that *Trpm2*$^+$ *Vglut2*$^+$ POA neurons detect increased body temperature and initiate thermoregulatory defense mechanisms, putatively through activation of stress-responsive *Crh*$^+$ neurons in the PVH (Fig. 4G).

Discussion

Explanations of the molecular mechanisms mediating thermal detection in preoptic WSNs have remained speculative (*57*, *58*). We identified TRPM2 as a thermal sensor in a subset of POA neurons that are part of a circuit controlling T_{core}.

Preoptic TRPM2 was activated at temperatures above the physiological set point of 37°C, arguing for a function of this receptor at conditions of elevated core temperatures and heat stress. Our results demonstrate a role for preoptic TRPM2 in regulating the magnitude of the fever response, suggesting that heightened temperatures, potentially

together with reactive oxygen species that are produced under these conditions (*59*), activate the channel to promote heat loss and prevent overheating.

Fever temperatures activate the immune system to modulate inflammatory responses (*60*). TRPM2 is expressed in the immune system (*61*), suggesting that fever-activated TRPM2 might modulate immune cell function. TRPM2 activity has been shown to inhibit and counteract inflammatory (pyrogenic) signaling in phagocytes (*62*), paralleling our results and emphasizing a convergent TRPM2-based mechanism used by both the immune and nervous systems to limit the extent of an inflammatory response and the mediation of antipyresis.

We observed a TRPM2-mediated reduction in T_{core} only when strong fever responses were induced, suggesting that TRPM2 limits the upper fever range and acts as an "emergency break" to prevent overheating and tissue damage. Alternatively, it is possible that TRPM2 plays a more prominent role in fever regulation, but that this function is masked by compensatory mechanisms triggered in *Trpm2*$^{-/-}$ mice that ubiquitously lack this ion channel throughout development.

The current model of thermoregulation predicts that the action potential firing rate of WSNs in the POA underlies T_{core} homeostasis and controls peripheral autonomous thermal responses (*3*). We found that chemogenetic activation and inhibition of *Trpm2*$^{+}$ WSNs in mice results in hypo- and hyperthermia, respectively, providing direct in vivo evidence for the validity of this hypothesis.

Twenty to 40% of POA neurons are sensitive to temperature and respond to stimuli around 37°C in electrophysiological experiments (*17*). Using calcium imaging, we found that only around 16% of neurons responded to a temperature increase. It is possible that our approach only allowed the detection of neurons that robustly responded to a thermal stimulus. Buffering of intracellular free calcium by the calcium indicators used in our experiments is one possible explanation for the reduced sensitivity and might explain the lower percentage of responsive neurons. Our data indicate that the TRPM2 receptor is unlikely to account for temperature sensitivity at normothermia but rather detects heat stress above 37°C. Accordingly, in POA brain slices, some thermal responses were still detectable in the absence of TRPM2, implying that additional mechanisms mediate preoptic responses to warming. Given the relatively broad expression of TRPM2 in the POA, it is plausible that the receptor covers detection of the upper, pathological temperature range in many or even all WSNs.

Previous single-cell transcriptome analysis has shown that preoptic WSNs are unexpectedly heterogeneous (*63*). Nevertheless, WSNs have been found to largely be inhibitory (GABAergic) neurons, which is in agreement with our histochemical analysis (summarized in fig. S4A). However, because the hypothermic phenotype that we observed in *Trpm2-Cre* mice was recapitulated by activating the smaller subpopulation of excitatory *Vglut2*$^{+}$ neurons but not by activating inhibitory (*Vgat*$^{+}$) neurons, we focused on the excitatory branch of the *Trpm2*$^{+}$ population. We found that preoptic *Vglut2*$^{+}$ neurons project to and excite *Crh*$^{+}$ neurons in the PVH, a hypothalamic cell population that is not primarily associated with thermoregulation (*3*), but rather controls stress reactions including fever responses by activation of the HPA axis. Excitation of PVH neurons inhibits PGE_2-induced fever (*47*). Moreover, corticosterone release by HPA axis activation has been found to counteract and reduce fever responses (*64*, *65*). These findings are in agreement with our data. The TRPM2 receptor may curtail PGE_2-triggered fever and induce hypothermia by mediating monosynaptic excitation of *Crh*$^{+}$ neurons in the PVH through an excitatory thermoregulatory pathway that connects the POA with the HPA axis.

Our study delineates a genetic framework for dissecting the central pathways controlling temperature homeostasis and provides a way to remotely control core body temperature in conscious, unrestrained mice by chemogenetic manipulation of the hypothalamic thermostat. These hypo- and hyperthermic model systems may help in exploring the effects of altered core body temperature on diverse processes such as trauma recovery, immune modulation, energy expenditure, obesity, and longevity.

REFERENCES AND NOTES

1. T. Bartfai, B. Conti, *Sci. World J.* **10**, 490–503 (2010).
2. C. B. Saper, A. A. Romanovsky, T. E. Scammell, *Nat. Neurosci.* **15**, 1088–1095 (2012).
3. S. F. Morrison, *Auton. Neurosci.* **196**, 14–24 (2016).
4. M. E. Musselman, S. Saely, *Am. J. Health Syst. Pharm.* **70**, 34–42 (2013).
5. W. D. Dietrich, H. M. Bramlett, *Brain Res.* **1640**, 94–103 (2016).
6. T. C. Wu, J. C. Grotta, *Lancet Neurol.* **12**, 275–284 (2013).
7. T. L. Horvath, N. S. Stachenfeld, S. Diano, *Yale J. Biol. Med.* **87**, 149–158 (2014).
8. H. C. Heller, L. I. Crawshaw, H. T. Hammel, *Sci. Am.* **239**, 102–110, 112–113 (1978).
9. B. A. Baldwin, D. L. Ingram, *J. Physiol.* **191**, 375–392 (1967).
10. H. T. Hammel, J. D. Hardy, M. M. Fusco, *Am. J. Physiol.* **198**, 481–486 (1960).
11. H. W. Magoun, F. Harrison, J. R. Brobeck, S. W. Ranson, *J. Neurophysiol.* **1**, 101–114 (1938).
12. E. Satinoff, *Am. J. Physiol.* **206**, 1389–1394 (1964).
13. B. Folkow, G. Strom, B. Uvnas, *Acta Physiol. Scand.* **17**, 317–326 (1949).
14. B. Conti *et al.*, *Science* **314**, 825–828 (2006).
15. M. M. Fusco, J. D. Hardy, H. T. Hammel, *Am. J. Physiol.* **200**, 572–580 (1961).
16. H. C. Heller, *Experientia Suppl.* **32**, 267–276 (1978).
17. J. A. Boulant, *J. Appl. Physiol.* **100**, 1347–1354 (2006).
18. T. Nakayama, J. S. Eisenman, J. D. Hardy, *Science* **134**, 560–561 (1961).
19. T. Nakayama, H. T. Hammel, J. D. Hardy, J. S. Eisenman, *Am. J. Physiol.* **204**, 1122–1126 (1963).
20. A. E. Oliver, G. A. Baker, R. D. Fugate, F. Tablin, J. H. Crowe, *Biophys. J.* **78**, 2116–2126 (2000).
21. C. Cai, X. Meng, J. He, H. Wu, F. Zou, *Neurosci. Lett.* **506**, 336–341 (2012).
22. I. V. Tabarean, B. Conti, M. Behrens, H. Korn, T. Bartfai, *Neuroscience* **135**, 433–449 (2005).
23. J. A. Boulant, J. B. Dean, *Annu. Rev. Physiol.* **48**, 639–654 (1986).
24. R. Palkar, E. K. Lippoldt, D. D. McKemy, *Curr. Opin. Neurobiol.* **34**, 14–19 (2015).
25. J. Vriens, B. Nilius, T. Voets, *Nat. Rev. Neurosci.* **15**, 573–589 (2014).
26. H. Wang, J. Siemens, *Temperature* **2**, 178–187 (2015).
27. L. Vay, C. Gu, P. A. McNaughton, *Br. J. Pharmacol.* **165**, 787–801 (2012).
28. H. Z. Hu *et al.*, *J. Biol. Chem.* **279**, 35741–35748 (2004).
29. K. Togashi, H. Inada, M. Tominaga, *Br. J. Pharmacol.* **153**, 1324–1330 (2008).
30. S. Z. Xu *et al.*, *Br. J. Pharmacol.* **145**, 405–414 (2005).
31. D. M. Bautista *et al.*, *Nature* **448**, 204–208 (2007).
32. A. Dhaka *et al.*, *Neuron* **54**, 371–378 (2007).
33. K. Zimmermann *et al.*, *Proc. Natl. Acad. Sci. U.S.A.* **108**, 18114–18119 (2011).
34. B. Xiao, B. Coste, J. Mathur, A. Patapoutian, *Nat. Chem. Biol.* **7**, 351–358 (2011).
35. J. Siemens *et al.*, *Nature* **444**, 208–212 (2006).
36. D. E. Clapham, C. Montell, G. Schultz, D. Julius, *Pharmacol. Rev.* **55**, 591–596 (2003).
37. J. Vriens *et al.*, *Neuron* **70**, 482–494 (2011).
38. M. Kashio *et al.*, *Proc. Natl. Acad. Sci. U.S.A.* **109**, 6745–6750 (2012).
39. A. L. Perraud *et al.*, *Nature* **411**, 595–599 (2001).
40. Y. Sano *et al.*, *Science* **293**, 1327–1330 (2001).
41. S. Yamamoto *et al.*, *Nat. Med.* **14**, 738–747 (2008).
42. W. P. Cheshire Jr., *Auton. Neurosci.* **196**, 91–104 (2016).
43. K. Togashi *et al.*, *EMBO J.* **25**, 1804–1815 (2006).
44. T. W. Chen *et al.*, *Nature* **499**, 295–300 (2013).
45. F. Tronche *et al.*, *Nat. Genet.* **23**, 99–103 (1999).
46. M. Lazarus *et al.*, *Nat. Neurosci.* **10**, 1131–1133 (2007).
47. C. J. Madden, S. F. Morrison, *Am. J. Physiol. Regul. Integr. Comp. Physiol.* **296**, R831–R843 (2009).
48. T. E. Scammell, J. K. Elmquist, J. D. Griffin, C. B. Saper, *J. Neurosci.* **16**, 6246–6254 (1996).
49. L. M. Harden, I. du Plessis, S. Poole, H. P. Laburn, *Brain Behav. Immun.* **22**, 838–849 (2008).
50. B. L. Roth, *Neuron* **89**, 683–694 (2016).
51. M. Koch *et al.*, *Nature* **519**, 45–50 (2015).
52. R. M. McAllen, M. Tanaka, Y. Ootsuka, M. J. McKinley, *Eur. J. Appl. Physiol.* **109**, 27–33 (2010).
53. C. J. Gordon, *Temperature Regulation in Laboratory Rodents* (Cambridge Univ. Press, 1993).
54. L. Vong *et al.*, *Neuron* **71**, 142–154 (2011).
55. L. Borgius, C. E. Restrepo, R. N. Leao, N. Saleh, O. Kiehn, *Mol. Cell. Neurosci.* **45**, 245–257 (2010).
56. Y. Matsuoka *et al.*, *Proc. Natl. Acad. Sci. U.S.A.* **100**, 4132–4137 (2003).
57. J. A. Boulant, *Am. J. Physiol. Regul. Integr. Comp. Physiol.* **290**, R1481–R1484, discussion R1484 (2006).
58. S. Kobayashi, A. Hori, K. Matsumura, H. Hosokawa, *Am. J. Physiol. Regul. Integr. Comp. Physiol.* **290**, R1479–R1480, discussion R1484 (2006).
59. W. Riedel, G. Maulik, *Mol. Cell. Biochem.* **196**, 125–132 (1999).
60. S. S. Evans, E. A. Repasky, D. T. Fisher, *Nat. Rev. Immunol.* **15**, 335–349 (2015).
61. H. Knowles, Y. Li, A. L. Perraud, *Immunol. Res.* **55**, 241–248 (2013).
62. A. Di *et al.*, *Nat. Immunol.* **13**, 29–34 (2012).
63. J. Eberwine, T. Bartfai, *Pharmacol. Ther.* **129**, 241–259 (2011).
64. I. Chowers, N. Conforti, S. Feldman, *Am. J. Physiol.* **214**, 538–542 (1968).
65. J. L. McClellan, J. J. Klir, L. E. Morrow, M. J. Kluger, *Am. J. Physiol.* **267**, R705–R711 (1994).

ACKNOWLEDGMENTS

We thank Y. Mori for *Trpm2*$^{-/-}$ mice and TRPM2 antisera; B. Lowell for *Vgat-Cre* mice; members of R. Kuner's laboratory, the Nikon Imaging Center, and V. Grinevich for sharing reagents, equipment, and expertise; A. von Seggern and C. Steinmeyer-Stannek for technical support; K. Schrenk-Siemens, W. de Lima, and P. Bengtson for help with calcium imaging; and C. Bohlen and A. Littlewood-Evans for criticism and reading of the manuscript. All data necessary to understand the study and its conclusions are in the body of the manuscript and in the supplementary materials. All primary data are archived on secure servers at the University Hospital Heidelberg. All data will be made available upon request. This work was supported by the European Research Council (grant ERC-2011-StG-280565 to J.S.), the Alexander von Humboldt Foundation (German Federal Ministry for Education and Research, BMBF; fellowship to G.B.K. and grant to J.S.), and the German Research Foundation (grants as part of the Collaborative Research Center SFB-1158 to P.H. and J.S.). Additional support came from the CellNetworks Cluster of Excellence. J.S., together with K.S., H.Wa., and G.B.K., conceived the project and designed the experiments. K.S. designed and conducted the cellular screen and analysis; J.P. designed and performed electrophysiological experiments; G.B.K. conceived the slice physiology and fever experiments; and H.Wa. conceived and conducted the chemogenetic experiments and, together with H.We., P.H., and F.d.C.R., generated *Trpm2-Cre* mice. H.We. and H.Wa. conducted histochemical analysis. J.S. wrote the paper. All authors commented on and approved the paper.

SUPPLEMENTARY MATERIALS

www.sciencemag.org/content/353/6306/1393/suppl/DC1
Materials and Methods
Figs. S1 to S4
Table S1
References (*66*–*76*)
Movie S1

24 March 2016; accepted 27 July 2016
Published online 25 August 2016
10.1126/science.aaf7537

The TRPM2 channel is a hypothalamic heat sensor that limits fever and can drive hypothermia

Kun Song, Hong Wang, Gretel B. Kamm, Jörg Pohle, Fernanda de Castro Reis, Paul Heppenstall, Hagen Wende and Jan Siemens

Science **353** (6306), 1393-1398.
DOI: 10.1126/science.aaf7537originally published online August 25, 2016